0^+ to 0^- transition in the $^{16}O(p,n)^{16}F$ reaction at 79 MeV

R. Madey,[1,2] B. S. Flanders,[1,3] B. D. Anderson,[1] A. R. Baldwin,[1] W. Bertozzi,[4] T. Chittrakarn,[1] J. R. Comfort,[5] J. M. Finn,[6] C. C. Foster,[7] C. Hyde-Wright,[8] J. J. Kelly,[9] C. Lebo,[1] H. Orihara,[10] W. Pairsuwan,[1] and J. W. Watson[1]

[1]*Department of Physics, Kent State University, Kent, Ohio 44242*
[2]*Department of Physics, Hampton University, Hampton, Virginia 23668*
[3]*Department of Physics, The American University, Washington, D.C. 20016*
[4]*Department of Physics, Massachusetts Institute of Technology, Cambridge, Massachusetts 02139*
[5]*Department of Physics, Arizona State University, Tempe, Arizona 85287*
[6]*Department of Physics, College of William and Mary, Williamsburg, Virginia 23185*
[7]*Indiana University Cyclotron Facility, Bloomington, Indiana 47405*
[8]*Department of Physics, Old Dominion University, Norfolk, Virginia 23529*
[9]*Department of Physics, University of Maryland, College Park, Maryland 20742*
[10]*Cyclotron and Radioisotope Center, Tohoku University, Sendai 980, Japan*

(Received 5 August 1997)

The isovector 0^+ to 0^- transition in the $^{16}O(p,n)^{16}F$ (g.s.) reaction was studied at 79 MeV. Differential cross sections were extracted for the transitions to the low-lying complex of 0^-, 1^-, 2^-, and 3^- states in ^{16}F at 12 laboratory angles from 0.3° to 63° which correspond to momentum transfers from 0.21 to 2.0 fm^{-1}. An energy resolution of 140 keV (FWHM) was achieved which was sufficient to separate the yields for each of these four states. Distorted-wave-impulse-approximation (DWIA) calculations were performed and compared with the extracted cross sections for these four transitions. The DWIA calculations with the effective interaction of Franey and Love provide a good description of the experimental measurements for the 0^- transition at low momentum transfer, but overestimate the data at larger momentum transfer. The experimental results for the 1^-, 2^-, and 3^- transitions are described reasonably well by the DWIA calculations. [S0556-2813(97)02412-6]

PACS number(s): 25.40.Ep, 27.20.+n, 25.40.Kv

I. INTRODUCTION

The excitation of isovector $J^\pi = 0^-$ transitions from a 0^+ ground state is of interest in nuclear physics because, in the absence of optical distortions, such transitions are sensitive only to the longitudinal $(\vec{\sigma}\cdot\vec{q})$ spin response of nuclei and not to the transverse $(\vec{\sigma}\times\vec{q})$ response. The (p,n) reaction is a favorable probe of these transitions because it proceeds predominantly through a one-step process and excites only the isovector states in the final nucleus; in contrast, these transitions are difficult to observe with the (p,p') reaction because the background isoscalar transitions overwhelm the relatively weak, high-lying, isovector excitations. Electroexcitation of a $0^+ \rightarrow 0^-$ transition is forbidden to first order because of the transverse character of the one-photon exchange. Excitation of longitudinal-spin transitions is forbidden also by particles with zero spin such as pions and alpha particles. Thus, charge-exchange reaction studies of isovector 0^- transitions are expected to provide information that is difficult to obtain from other sources.

The nucleon-nucleus scattering operator for the 0^+ to 0^- transition excited via the (p,n) reaction is given by [1]

$$M = A\vec{\sigma}_p\cdot\vec{q} + B\vec{\sigma}_p\cdot\vec{Q}, \tag{1}$$

where

$$\vec{Q} = \vec{k}_i + \vec{k}_f \tag{2}$$

in the adiabatic limit (Q value = 0), and

$$\vec{q} = \vec{k}_i - \vec{k}_f. \tag{3}$$

Here k_i (k_f) is the initial (final) relative momentum, $\vec{\sigma}_p$ is the Pauli spin operator of the incident proton, and the quantities A and B are scalar functions of the other dynamical variables of the system. In principle, the quantities A and B can be obtained from the dependence of the differential cross section on the momentum transfer q. The functions A and B are the inelastic scattering counterparts to the spacelike and timelike couplings in β decay [2].

Much theoretical and experimental interest has been focused upon transitions with pionlike quantum numbers $(0^-, 1^+, 2^-, \ldots)$, largely because phenomena involving the pion field in nuclei should be most evident in these transitions. Because the isovector 0^+ to 0^- transition is characterized by these pionlike quantum numbers ($\Delta S = \Delta T = 1$), it should be sensitive to the effects of the pion field in nuclei. On general grounds, the 0^- transition is expected to be more sensitive to pionic effects than higher multipoles; however, there have been few measurements of 0^-, $T=1$ transitions. Reaction studies of such transitions should provide unique information on pion-exchange currents at large momentum transfers.

The isovector 0^- transition in the mass-16 system was observed with β decay [3], μ capture [4], and low-energy (p,n) [5] and (p,p') [6] experiments. The β-decay and μ-capture measurements are less sensitive to the pionic effects because the momentum transfer ($q \leqslant 0.5$ fm^{-1}) is relatively small. The (p,n) cross sections at 35 MeV [5] covered

a range of momentum transfer q from 0.34 to 2.0 fm^{-1}; for $q \geq 1.4$ fm^{-1}, the measured cross section exceeded that calculated in the distorted-wave-impulse approximation (DWIA) with the M3Y effective interaction [7]. This enhancement was attributed to pionic effects. Orihara *et al.* [8] measured the angular distributions of the $1/2^-$ to $1/2^+$ and 1^+ to 1^- transitions (with $\Delta J=0$ and $\Delta\pi=-1$) in the $^{13}C(p,n)$ and $^{14,15}N(p,n)$ reactions at 35 MeV in order to obtain additional information equivalent to that from the 0^+ to 0^- transitions.

Both the isovector and isoscalar 0^+ to 0^- transitions were measured with the $^{16}O(\vec{p},p')$ reaction at 65 MeV over the momentum transfer range from 0.3 to 1.6 fm^{-1}. The discrepancy observed between the measured cross sections and those calculated in the DWIA with the M3Y effective interaction for the isovector transition at 35 MeV was not observed in the $(\vec{p},p')$ experiment at 65 MeV. The difference between the results at 35 MeV and 65 MeV indicates that more complicated reaction mechanisms may be required to describe these data.

Higher incident energies would provide a simpler and better understood reaction mechanism; however, in order to resolve the 0^- ground-state transition from the 1^- transition at 190 keV in a (p,n) experiment, we determined 80 MeV to be the highest proton energy that would permit us to resolve this state with the neutron time-of-flight facility available at the Indiana University Cyclotron Facility (IUCF). Although the 0^- transition is of primary interest, we extracted also the cross sections to the 1^-, 2^-, and 3^- states which, together with the 0^- ground state, form a low-lying complex in ^{16}F. DWIA calculations were performed and compared with the experimental results for all four of these transitions. The transition to the 0^- state is compared also with the analog (p,p') transition measurements at 65 MeV.

II. EXPERIMENTAL PROCEDURE

Long flight paths ($\sim$130 m) were required to achieve the energy resolution ($\leq$150 keV) necessary to separate the four low-lying states in ^{16}F. In order to eliminate the large ''wraparound'' background which would arise from the long flight paths and typical pulse selection at the IUCF, the ''stripper loop'' [9] was used to increase the beam-pulse spacing. Briefly, the stripper loop is a ring which stores the beam pulses for later delivery all at once. This method of increasing the pulse spacing reduces the loss of current associated with traditional pulse selection. For these measurements, a pulse selection of 1 in 72 was employed. The removal of the wraparound background increased the importance of reducing the background from cosmic rays as discussed below. The wraparound background arises from slow neutrons from earlier beam bursts.

We measured neutron time-of-flight (TOF) spectra from 79-MeV protons on a Mylar $(C_{10}H_8O_4)_n$ target ($\sim$10.6 mg/cm^2 thick). Because the Q value for the $^{12}C(p,n)^{12}N$ reaction is -18.1 MeV and that for the $^{16}O(p,n)^{16}F$ reaction is -16.2 MeV, there is a 1.9 MeV region of excitation in ^{16}F that is free of ^{12}N peaks from the (p,n) reaction on the ^{12}C in the Mylar target. The states of interest here are in this region.

Neutron detector arrays were installed in three stations at 0°, 24°, and 45° with respect to the undeflected proton beam at distances of 131, 133, and 131 m, respectively, from the target. The arrays were comprised of NE-102 plastic scintillators 0.101-m thick. Three 1.02-m long by 0.51-m high detectors with a combined frontal area of 1.55 m^2 were located in the 0° station; one 0.51-m high and one 1.02-m high detector, both 1.02-m long, with a combined frontal area of 1.55 m^2 were located in the 24° station; and two 1.52-m long by 0.76-m high detectors with a combined frontal area of 2.32 m^2 were located in the 45° station. The performance of the large-volume, mean-timed, neutron detectors was reported previously [10]. Thin (0.953- and 1.27-cm thick) plastic NE-102 or NE-114 scintillation counters were placed above, in front of, behind, and below the neutron detectors to veto events arising from cosmic rays. The addition of anticoincidence counters behind and below the detector arrays reduced the background from cosmic-ray events nearly fourfold. An absorber was placed between each detector and the rear anticoincidence counter to stop recoil protons from neutron interactions in the rear of the detectors from reaching the anticoincidence counters; the absorber was 3.8 cm of Lexan for the 0° and 24° stations, and 15 cm of plywood for the 45° station.

In order to calculate reliably the neutron detection efficiency, the pulse-height response of each neutron detector was obtained with the 2.61-MeV gamma ray from a ^{228}Th radioactive source. The efficiency was checked (to an accuracy of $\sim$10%) by verifying that the 0° cross section for the $^{12}C(p,n)^{12}N$ (g.s.) reaction (measured with a ^{12}C target enriched to 99.9%) was consistent with earlier measurements [11–13] at 62, 99, 120, 135, and 160 MeV. This measured ^{12}N g.s. cross section served to normalize the yields from the Mylar targets which were prone to damage from the proton beam. The heating of the Mylar by the beam tended to reduce the target thickness. Also, the relative amounts of ^{12}C and ^{16}O in the target was altered by the boiling off of oxygen. To compensate for the loss of oxygen, targets were changed frequently; moreover, the ratio of the yields from the ground state in ^{12}N and the 2^- state in ^{16}F, measured for short periods on new targets, was used as a normalization.

Time-of-flight spectra were recorded at twelve laboratory

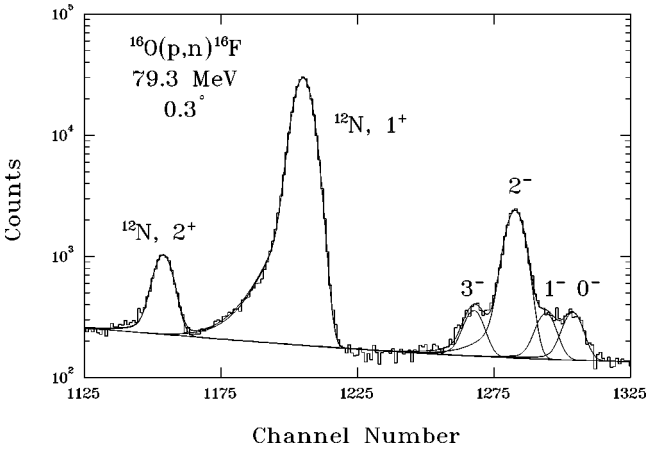

FIG. 1. Time-of-flight (TOF) spectrum at 0.3° from the $^{16}O(p,n)^{16}F$ reaction at 79 MeV. The solid curve is a fit to the observed spectrum.

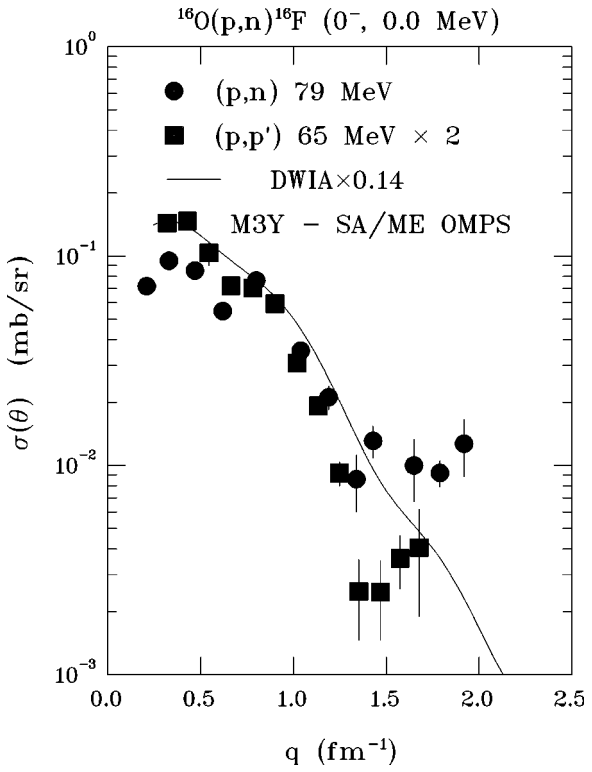

FIG. 2. Comparison of the momentum-transfer distributions of the differential cross sections measured for the transitions to the 0^- ground state in ^{16}F from the ^{16}O$(p,n)^{16}$F reaction at 79 MeV and to the analog 0^- state at 12.80 MeV in ^{16}O from the ^{16}O(p,p') reaction at 65 MeV. The curve represents a DWIA calculation (see text).

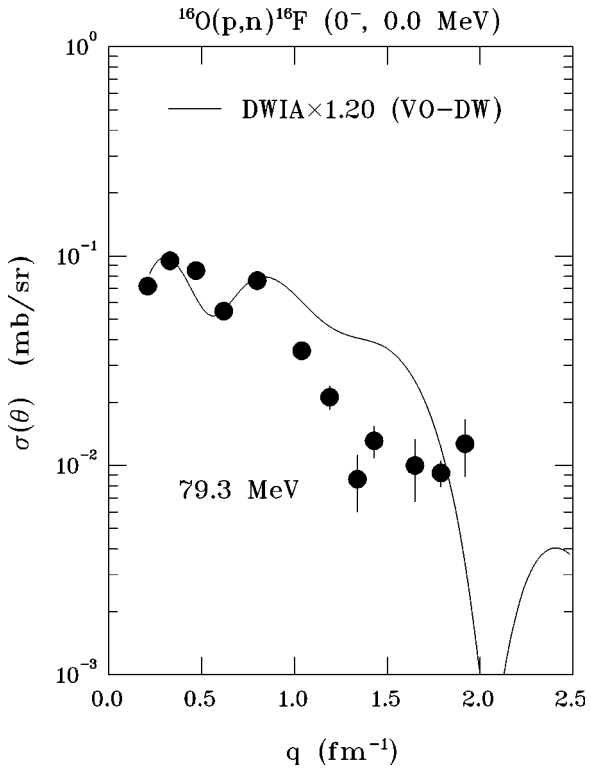

FIG. 3. Momentum-transfer distribution of the differential cross section measured for the transition to the 0^- ground state in ^{16}F from the ^{16}O$(p,n)^{16}$F reaction at 79 MeV. The curve represents a DWIA calculation (see text).

angles in the range from 0.3° to 63°; these angles correspond to momentum transfers from 0.21 to 2.0 fm^{-1}. Presented in Fig. 1 is the spectrum measured at 0.3°; this spectrum shows the four low-lying states in ^{16}F and two low-lying states in ^{12}N. The energy resolution, measured as the FWHM of the ^{12}N ground state, was 142 keV at a detector threshold of 25 MeV of equivalent-electron energy. The yield for each of the four low-lying ^{16}F states was extracted with a peak-fitting code which utilized the peak shape from the ^{12}N ground state and fixed the excitation energies of the peaks to their known values. The fit to the time-of-flight spectrum at 0.3° is shown in Fig. 1. The fitting procedure and data analysis are described in more detail in Ref. [14]. The momentum-transfer distribution of the differential cross section for the transitions to the 0^-, 1^-, 2^-, and 3^- states in this low-lying complex are presented in Table 1 and Figs. 2–6.

III. RESULTS AND DISCUSSION

Listed in Table I are the differential cross section distributions for the transitions to the 0^-, 1^-, 2^-, and 3^- states in ^{16}F. In Fig. 2 we show the comparison of the ^{16}O$(p,n)^{16}$F(0^-, g.s.) data from this work with the analog ^{16}O$(p,p')^{16}$O(0^-, 12.80 MeV) data from Hosono *et al.* [6] at 65 MeV. Shown also are DWIA calculations similar to those presented by Hosono *et al.* for comparison with the (p,p') data. The calculations were performed with the impulse approximation code DW81 due to Schaeffer and Raynal

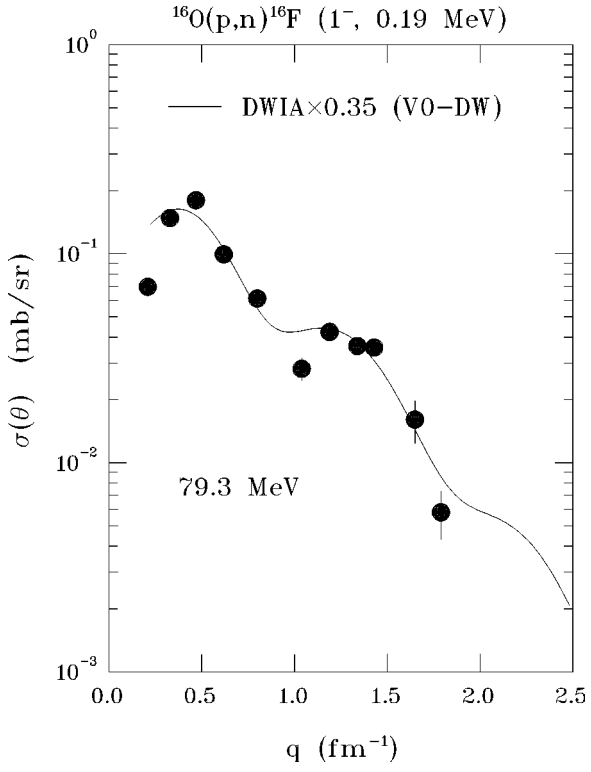

FIG. 4. Momentum-transfer distribution of the differential cross section measured for the transition to the 1^- state at 0.19 MeV in ^{16}F from the ^{16}O$(p,n)^{16}$F reaction at 79 MeV. The curve represents a DWIA calculation (see text).

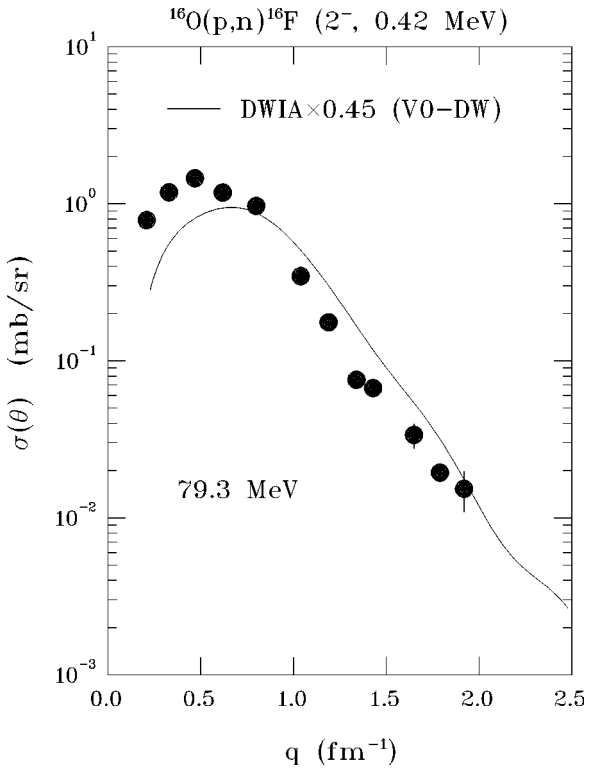

FIG. 5. Momentum-transfer distribution of the differential cross section measured for the transition to the 2^- state at 0.42 MeV in ^{16}F from the $^{16}O(p,n)^{16}F$ reaction at 79 MeV. The curve represents a DWIA calculation (see text).

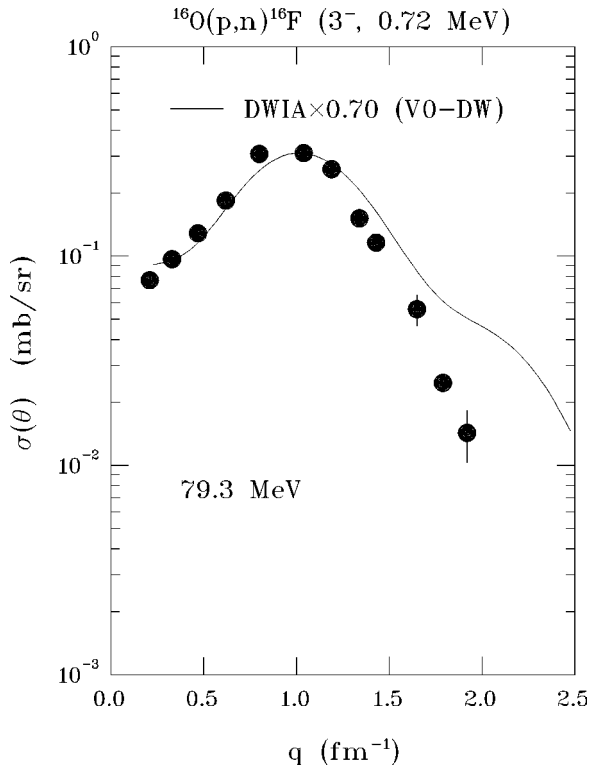

FIG. 6. Momentum-transfer distribution of the differential cross section measured for the transition to the 3^- state at 0.72 MeV in ^{16}F from the $^{16}O(p,n)^{16}F$ reaction at 79 MeV. The curve represents a DWIA calculation (see text).

as extended by Comfort [15]. The optical potentials assumed were of the form

$$V(r)=V_{\rm Coul}-V_R f(r;r_R,a_R)-iWf(r;r_W,a_W) +iW_S df(r;r_{Ws},a_{Ws})/dr +(V_{LS}(1/r)df(r;r_{LS},a_{LS})/dr)(\vec{L}\cdot\vec{S}), \quad (4)$$

where

$$f(r;r_0,a_0)=\{1+\exp[(r-r_0A^{1/3})/a_0]\}^{-1}. \quad (5)$$

In Eq. (4) $V_{\rm Coul}$ is the Coulomb potential for a uniformly charged sphere of radius $1.25A^{1/3}$ fm. The quantity V_R denotes the strength of the real central potential, while W and W_S are the strengths of the volume and surface parts, respectively, of the imaginary central potential. The quantity $V_{\rm LS}$ is the strength of the real spin-orbit potential. The Woods-Saxon form factor is defined in Eq. (5) in terms of the radius and diffuseness parameters r_0 and a_0, respectively.

The calculations presented in Fig. 2 use an optical parameter set for the entrance channel at 65 MeV taken from Sakaguchi *et al.* [16] and a set for the exit channel at 52.5 MeV from the systematic analysis by Menet *et al.* [17]. The parameters for these potentials are presented in Table II. Single-particle wave functions in the form factor were calculated in a Woods-Saxon well with $r_0=1.25$ fm, $a_0=0.65$ fm, plus a Thomas-type spin-orbit potential with $V_{\rm SO}=6.0$ MeV. The initial state wave function is taken to be a closed shell for the ^{16}O target nucleus and the final state wave function to be the simple $(2s_{1/2},\ 1p_{1/2}{}^{-1})$ particle-hole state. Although the $2s_{1/2}$ particle state is unbound, it was assumed here to be bound by 0.05 MeV in the Woods-Saxon potential. The nucleon-nucleon (NN) effective interaction assumed was the M3Y interaction of Bertsch *et al.* [7], which was found to describe successfully various reactions at 40 to 65 MeV.

As seen in Fig. 2, the (p,n) and analog (p,p') data (multiplied by a factor of 2 for isospin geometrical factors) generally agree. The (p,n) data are somewhat less forward peaked and show a more pronounced diffraction minimum near 0.6 fm^{-1}. The DWIA calculation generally describes the (p,p') data with a normalization factor of 0.12, but does not reproduce the diffraction minimum seen in the (p,n) data. The comparison with the (p,p') data is similar to that presented by Hosono *et al.*

In Figs. 3–6, we show the (p,n) data from this work for the 0^-, 1^-, 2^-, and 3^- transitions, respectively. We compare these distributions with DWIA calculations which use unbound form factors for the final particle states and optical-model parameters for elastic scattering on ^{16}O at the appropriate energies for the (p,n) data. The optical-model parameters were taken from the work of van Oers and Cameron [18] for fits to elastic scattering on ^{16}O from 23 to 100 MeV and are presented in Table II. This study included measurements at 66 and 100 MeV, which were interpolated to provide parameters at 79 MeV for the entrance channel. The 66-MeV parameters were used for the exit channel. The calculations assume Woods-Saxon form factors for the nuclear structure wave functions identical to those described above for the calculations of Fig. 2. The NN effective interaction is taken to be that of Franey and Love at 100 MeV [19]. The sd-shell final-state particle wave functions were calculated

TABLE I. Differential cross sections for the transitions to the 0^-, 1^-, 2^-, and 3^- states at 0.0, 0.19, 0.42, and 0.72 MeV, respectively, in ^{16}F with the ^{16}O(p,n) reaction at 79.3 MeV.

$\theta_{\text{c.m.}}$ deg	q fm^{-1}	0^- σ (mb/sr)	1^- σ (mb/sr)	2^- σ (mb/sr)	3^- σ (mb/sr)
0.3	0.21	0.072(5)	0.070(4)	0.787(10)	0.077(4)
8.6	0.33	0.095(5)	0.148(6)	1.183(13)	0.097(5)
14.0	0.47	0.085(3)	0.180(4)	1.454(07)	0.128(4)
19.4	0.62	0.055(3)	0.099(3)	1.178(07)	0.184(4)
25.8	0.80	0.076(3)	0.061(4)	0.968(08)	0.308(5)
34.3	1.04	0.035(3)	0.028(3)	0.346(06)	0.311(9)
39.6	1.19	0.021(3)	0.042(3)	0.176(04)	0.260(7)
44.9	1.34	0.009(3)	0.036(3)	0.076(03)	0.152(6)
48.1	1.43	0.013(3)	0.036(3)	0.067(03)	0.116(3)
56.5	1.65	0.010(3)	0.016(4)	0.034(06)	0.056(9)
61.7	1.79	0.009(2)	0.006(2)	0.019(02)	0.025(2)
66.9	1.92	0.013(4)		0.015(04)	0.014(4)

by using the unbound form factor option in the code DW81. A closed p shell is assumed for the ^{16}O target nucleus and the final states include all possible one-particle–one-hole excitations from the p shell to the sd shell. This prescription for the wave functions is the so-called Tamn-Dancoff approximation (TDA) and the calculation adopted here is that due to Donnelly and Walker [20].

We see in Fig. 3 that the DWIA calculations for the 0^- transition describe the data well at low-momentum transfer but overestimate the data at larger momentum transfer. A normalization factor of 1.2 is required in order to make the calculations agree with the data at low-momentum transfer. In order to test for sensitivity to the structure calculations, we tried different sets of wave functions for the 0^- transition. We used a shell-model calculation by Brown [21] that allows certain two-particle–two-hole excitations in the ^{16}O ground state and then one-particle–one-hole excitations built upon these states for the 0^- final state. These wave functions are expected to be more realistic than the simple TDA wave functions. We found little difference in the calculated cross sections for these wave functions. Also we tried other wave functions, including a calculation that uses the p-sd interaction of Millener and Kurath [22], and those of Gillet and Vinh Mau [23]; we see no significant differences with any of these different wave functions. In all of these shell-model calculations, the 0^- wave function is dominated by the $(2s_{1/2},1p_{1/2}{}^{-1})$ particle-hole configuration. The higher-lying $(1d_{3/2},1p_{3/2}{}^{-1})$ configuration mixes in very little, and the multiparticle-multihole configurations affect the 0^- wave function only slightly. Perhaps if one were to expand the model space to include $3\hbar\omega$ excitations, the wave function would be affected more.

The 1^-, 2^-, and 3^- transitions are described better than the 0^- transition by DWIA calculations which have the same ingredients as for the 0^- transition. The wave functions for the different final states were all obtained from the same TDA shell-model calculation [20]. For the 1^-, 2^-, and 3^- DWIA calculations, normalization factors less than unity are required in order to make the calculations agree with the data; this situation is customary for such calculations and is usually ascribed to the effects of multiparticle-multihole ground-state correlations and final-state configuration mixing which are not included in the simple TDA calculation. The 1^- transition is fit fairly well for shape over the entire range of momentum transfers studied. The 2^- calculation goes from underestimating the data at low momentum transfer to overestimating at higher momentum transfer. The 3^- calculation describes the data well at low-momentum transfers but overestimates the data at higher momentum transfer. We note that the ^{16}O$(p,n)0^-$ reaction is particularly sensitive to details of the interference between the $V_{\sigma\tau}$ and isovector tensor interactions; furthermore, two-step excitation via inelastic excitation of the ^{16}O$(3^-,T=0)$ state followed by charge exchange can substantially affect the energy dependence of this reaction. We conclude that significant improvement of the reaction model is needed to use the (p,n) reaction at low to intermediate energies to deduce the one-body spin-longitudinal matrix element for the 0^+ to 0^- transition.

TABLE II. Optical-model parameters. $r_C = 1.25$ fm.

E (MeV)	V_R (MeV)	r_R (fm)	a_R (fm)	W (MeV)	r_W (fm)	a_W (fm)	W_S (MeV)	r_{Ws} (fm)	a_{Ws} (fm)	V_{LS} (MeV)	r_{LS} (fm)	a_{LS} (fm)	Reference
65	27.17	1.30	0.66	12.85	0.28	1.20	4.94	1.35	0.38	23.17	1.06	0.58	Sakaguchi [16]
52	39.62	1.16	0.75	5.92	1.37	0.32	6.30	1.37	0.32	12.08	1.06	0.78	Menet [17]
79	30.19	1.24	0.65	4.87	1.76	0.64				24.96	1.02	0.64	van Oers [18]
66	36.14	1.17	0.73	6.74	1.58	0.40				24.80	1.11	0.58	van Oers [18]

IV. SUMMARY AND CONCLUSIONS

We observed the excitation of the 0^-, 1^-, 2^-, and 3^- states in ^{16}F via the $^{16}O(p,n)^{16}F$ reaction at an incident energy of 79 MeV and extracted momentum-transfer distributions of the differential cross section in the range $0.21 \leq q \leq 2.0$ fm^{-1}. The experimental results for the 0^- transition were compared with DWIA calculations that describe the data reasonably well at low momentum transfer but significantly overestimate the data at larger momentum transfer. These results contrast to those at 35 MeV of Orihara *et al.* [5] who see the experimental results at large momentum transfer to be much larger than IA calculation predictions, which was interpreted as a possible signature of meson-exchange currents (MEC's). For the $^{16}O(p,n)^{16}F(0^-,\text{g.s.})$ reaction, the large-momentum-transfer region is underestimated at 35 MeV and overestimated at 79 MeV. These discrepancies may be due to difficulties in the theoretical modeling of the reaction mechanism; it is known that IA calculations become more reliable for describing inelastic scattering only above about 100 MeV [24]. It is interesting that the experimental results of Hosono *et al.* [6] for the analog-state $^{16}O(p,p')^{16}O(12.797\ \text{MeV},0^-,T=1)$ reaction at 65 MeV agree generally with DWIA calculations from low to high momentum transfer. Prelimary results from measurements of $^{16}O(p,p')^{16}O(12.797\ \text{MeV},\ 0^-,\ T=1)$ at 200 MeV by Stephenson *et al.* [25] show good agreement at all momentum transfers with DWIA calculations for the cross sections, although analyzing powers are described poorly.

In this work, the 1^-, 2^-, and 3^- transitions are all described better by the same DWIA calculations, based on simple 1p-1h TDA final state wave functions. At this time, the description of the large-momentum-transfer region in the $^{16}O(p,n)^{16}F(0^-,\text{g.s.})$ reaction by impulse-approximation calculations is inconsistent; clearly measurements at energies above 100 MeV, where the impulse approximation is more reliable, would be desirable.

ACKNOWLEDGMENTS

This work was supported in part by the U.S. National Science Foundation and the U.S. Department of Energy.

[1] W. G. Love and J. R. Comfort, Phys. Rev. C **29**, 2135 (1984).
[2] I. S. Towner and F. C. Khanna, Nucl. Phys. **A372**, 331 (1981).
[3] C. A. Gagliardi, G. T. Garvey, J. R. Wrobel, and S. J. Freedman, Phys. Rev. Lett. **48**, 914 (1982).
[4] P. Guichon, B. Bihoreau, M. Giffon, A. Goncalves, J. Jolien, L. Roussel, and C. Samour, Phys. Rev. C **19**, 987 (1979).
[5] H. Orihara, S. Nishihara, K. Furukawa, T. Nadagawa, K. Maeda, K. Miura, and H. Ohnuma, Phys. Rev. Lett. **49**, 1318 (1982).
[6] K. Hosono, M. Fujiwara, K. Hatanaka, H. Ikegami, M. Kondo, N. Matsouka, T. Saito, S. Matsuki, K. Ogino, and S. Kato, Phys. Rev. C **30**, 746 (1984).
[7] G. F. Bertsch, J. Baryowicz, H. McManus, and W. G. Love, Nucl. Phys. **A284**, 399 (1977).
[8] H. Oirhara *et al.*, Phys. Lett. B **187**, 240 (1987).
[9] D. L. Friesel, R. E. Pollock, T. E. Ellison, and W. P. Jones, in *Tenth International Conference on Cyclotrons and their Applications*, East Lansing, Michigan, edited by F. Marti (IEEE Cat. No. 84-CH1996-3, IEEE, Piscataway, NJ, 1984), pp. 207–210; Nucl. Instrum. Methods **1310/11**, 864 (1985); IEEE Trans. Nucl. Sci. NS-**32**, 2691 (1985).
[10] R. Madey, J. W. Watson, M. Ahmad, B. D. Anderson, A. R. Baldwin, A. L. Casson, W. Casson, R. A. Cecil, A. Fazely, J. M. Knudson, C. Lebo, W. Pairsuwan, P. J. Pella, J. C. Varga, and T. R. Witten, Nucl. Instrum. Methods Phys. Res. **214**, 401 (1983).
[11] J. N. Knudson, B. D. Anderson, P. C. Tandy, J. W. Watson, and R. Madey, Phys. Rev. C **22**, 1826 (1980).
[12] B. D. Anderson, J. N. Knudson, R. Madey, and C. C. Foster, Nucl. Instrum. Methods **169**, 153 (1980).
[13] J. N. Knudson, Doctoral dissertation, Kent State University, 1980.
[14] B. S. Flanders, Doctoral dissertation, Kent State University, 1985.
[15] Program DWBA-81, J. R. Comfort, extended version of Program DWBA-70, R. Schaeffer and J. Raynal, Saclay Report No. CEA-R 4000, 1970 (unpublished).
[16] H. Sakaguchi, M. Nakamura, K. Hatanaka, A. Goto, F. Ohtani, H. Sakamoto, H. Ogawa, and S. Kobayashi, Phys. Rev. C **26**, 944 (1982).
[17] J. J. H. Menet, E. E. Gross, J. Malanify, and A. Zhuker, Phys. Rev. C **4**, 1114 (1971).
[18] W. T. H. van Oers and J. M. Cameron, Phys. Rev. **184**, 1061 (1969); (private communication).
[19] M. A. Franey and W. G. Love, Phys. Rev. C **31**, 488 (1985).
[20] T. W. Donnelly and G. E. Walker, Ann. Phys. (N.Y.) **60**, 209 (1970).
[21] B. A. Brown (private communication).
[22] D. J. Millener and D. Kurath, Nucl. Phys. **A255**, 315 (1975).
[23] V. Gillet and N. V. Mau, Nucl. Phys. **54**, 321 (1964).
[24] W. G. Love, A. Klein, M. A. Franey, and K. Nakayama, Can. J. Phys. **65**, 536 (1987).
[25] E. Stephenson, Indiana University Cyclotron Facility, IUCF Scientific and Technical report, 1989; (private communication).